中国光学 Chinese Optics 核心期刊

对史密斯–帕塞尔自由电子激光光栅的研究

孟现柱

引用本文:
孟现柱. 对史密斯–帕塞尔自由电子激光光栅的研究[J]. 中国光学, 2020, 13(2): 381–395. doi: 10.3788/CO.20201302.0381
MENG Xian–zhu. Study on grating of Smith–Purcell free–electron laser[J]. *Chinese Optics*, 2020, 13(2): 381–395. doi: 10.3788/CO.20201302.0381

在线阅读 View online: https://doi.org/10.3788/CO.20201302.0381

文章编号　2095-1531(2020)02-0381-15

Study on grating of Smith-Purcell free-electron laser

MENG Xian-zhu *
(*Shandong Provincial Key Laboratory of Optical Communication Science and Technology, School of Physics Science and Information Engineering, Liaocheng University, Liaocheng* 252059, *China*)
* *Corresponding author, E-mail: mengxz@ lcu. edu. cn*

Abstract: In order to study the relationship between the output frequency of Smith-Purcell free-electron laser and the depth, length and width of grating groove, the rectangular grating size of Smith-Purcell free-electron laser is discussed by means of theoretical analysis and particle simulation methods. First, by particle simulation, we found that the output frequency of Smith-Purcell free-electron laser decreases with the increase of grating groove depth, grating groove length and grating groove width. Then, the grating groove of Smith-Purcell free-electron laser is discussed by means of theoretical analysis. It is found that each grating groove can be equivalent to an LC resonant circuit. There are two kinds of radiation in Smith-Purcell free-electron laser, one is Smith-Purcell radiation and the other is LC oscillatory radiation. Finally, the LC oscillatory radiation of grating groove is estimated as well. It is found that the simulated values of output frequency of Smith-Purcell free-electron laser and the estimation values of LC oscillatory radiation of grating groove are both on the order of 10^2 GHz, and the variation is consistent. It is inferred that the output frequency of Smith-Purcell free-electron laser should be determined by grating groove rather than resonator.

Key words: physical electronics; free-electron laser; grating; resonator; Smith-Purcell radiation; LC resonance circuit

对史密斯-帕塞尔自由电子激光光栅的研究

孟现柱 *
(聊城大学物理科学与信息工程学院,山东省光通信科学与技术重点实验室,山东 聊城 252059)

摘要:为了研究史密斯 - 帕塞尔自由电子激光的输出频率和光栅槽深、光栅槽长、光栅槽宽的关系,对于基于矩形光栅的史密斯 - 帕塞尔自由电子激光利用粒子模拟软件进行模拟和理论分析。首先,利用粒子模拟软件模拟对于基于矩形光栅的史密斯 - 帕塞尔自由电子激光进行了研究,发现史密斯 - 帕塞尔自由电子激光的输出频率随光栅槽深、光栅槽长、光栅槽宽的增大而减少。接着,对史密斯 - 帕塞尔自由电子激光的光栅槽进行了理论分析,发现每个光栅槽都可以等效为一个 LC 谐振电路,并发现在史密斯 - 帕塞尔自由电子激光中存在两种辐射,一种是史密斯 - 帕塞尔辐射,另一种是 LC 振荡辐射。最后,对光栅槽的 LC 振荡辐射进行了估算,发现史密斯 - 帕塞尔自由电子激光输出频率的模拟值与光栅槽的 LC 振荡辐射估算值的数量级均为 10^2 GHz,且变化规律上一致。据此推测决定史密斯-帕塞尔自由电子激光输出频

收稿日期:2019-03-22;**修订日期**:2019-04-30
基金项目:国家自然科学基金资助项目(No. 11275089,No. 11375081)
Supported by National Natural Science Foundation of China (NSFC) (No. 11275089,No. 11375081)

率的应该是光栅槽,而不是谐振腔。

关　键　词:物理电子学;自由电子激光;光栅;谐振腔;史密斯-帕塞尔辐射;LC谐振电路

中图分类号:O463　　**文献标识码:**A　　doi:10.3788/CO.20201302.0381

1 Introduction

When an electron beam passes over the surface of a periodic metallic structure, it will excite electromagnetic radiation at far-infrared, micron, and terahertz bands. This phenomenon is known as Smith-Purcell (SP) effect, and this radiation is called Smith-Purcell Radiation (SPR)[1]. However, this spontaneous SPR is incoherent, weak and difficult to detect and apply. To generate coherent SPR, a relativistic electron beam is usually used to driven a high-frequency interaction system composed of an open (or closed) resonator as feedback element and a metal grating. This experimental structure is called Smith-Purcell Free-Electron Laser (SP FEL)[2-5]. The SP FEL has been successfully tested in the far-infrared, micron and terahertz bands[6-9]. These experiments have shown promising prospects for the development of light sources in the far-infrared, micron and terahertz bands, and have become one of the research hotspots of terahertz (THz, 0.1 ~ 10 THz) sources at home and abroad. They constitute a promising optional approach for developing high-power, high-frequency, tunable, more compact, simpler, and low-cost THz sources.

In order to generate high-power SP FEL, the researchers have studied how to optimize the resonator, electron beam and grating in recent years. The study on resonator optimization found that the open cavity structure similar to Orotron could increase the radiation power by more than two orders of magnitude[6]. The average power output at THz bands can reach hundreds of milliwatts or even a few watts, many orders of magnitude higher than the traditional Orotron. In terms of electron beam optimization, the SPR frequency and power can be improved by prebunching. In 2007, Shi Zongjun, Yang Ziqiang[9] *et al*. found that not only the coherent SPR can be generated, but also the desired SPR frequency and power can be obtain by prebunching. For example, coherent SPR can be obtained when a prebunched electron beam passes over the surface of a metal grating[10]. By selecting the right parameters, extremely strong narrow-band THz radiation can be generated. In 2016, Kumar P *et al*. reported the SP THz radiation generated by a laser-modulated electron beam on metal grating[11]. In terms of grating optimization, SPR is improved mainly by optimizing the grating shape and structure. In 2015, Naumenko *et al*. reported a kind of SPR based on concave grating, and found that the spatial density of coherent SPR could be significantly increased by concave grating. In the same year, Zhang P *et al*. also reported a kind of enhanced coherent THz SPR, which had been generated by optimizing the grating, prebunch and open resonator. In addition, they found that the order of magnitude of the starting current could be reduced by optimizing the grating parameters and changing the width and height of grating groove[12]. They also studied the enhanced THz SPR based on a grating groove array. The power of this SPR is ten times higher than that when electrons pass over a surface very close to the grating[13]. In 2016, Liu Weihao, Lu Yalin *et al*. proposed an improved SP FEL based on two cylindrical gratings in series. This improved SP FEL can increase the radiation frequency, and raise the radiation power by dozens of times[14-16]. It can be seen from above that in the study of SP FEL, the study of the relationship between the grating size and the output frequency of SP FEL has always been a blank. Therefore, in this paper, the SP FEL based on rectangular grating is taken as an example to study the relationship between the size of grating and the output frequency of SP FEL.

2　Structure and theory of the SP FEL based on rectangular grating

As illustrated in Fig. 1, the SP FEL structure based on rectangular grating consists of an electron gun, a resonator, a rectangular grating and a collector. In this device, at the resonator bottom is a rectangular grating, whose grooves are parallel to the x-axis direction. Both the grating and the resonator are made of metallic materials (such as oxygen-free copper) with good conductivity, so their surfaces can be considered as ideal conductors. The cathode (electron gun) on the left of the grating can produce a beam of electrons traveling along the z-axis. When the electron beam passes over the surface of the rectangular grating, a large number of charges will be induced on the grating surface to form a periodic electric field near the grating. Under the effect of the electric field, the electron beam in motion will emit SPR. The wavelength of SPR is

$$\lambda = \frac{D}{n}\left(\frac{1}{\beta} - \cos\theta\right), \tag{1}$$

where D is the grating period, n is the number of spatial harmonics, θ is the emission angle (that is, the angle between the SPR and the direction of electron motion), and β is the ratio of the velocity of electrons to the speed of light, $\beta = v/c$. According to the equation (1), the wavelength range of spontaneous SPR fundamental wave is from $D\left(\frac{1}{\beta} - 1\right)$ to $D\left(\frac{1}{\beta} + 1\right)$ [17-22]. According to traditional SP FEL theory, the resonator surface can reflect the SPR of various wavelengths back to the electron beams, and the reflected SPR can modulate the electron beams. However, at the initial stage of electron beam injection, the SPR is not strong enough to cause the electron beams to bunching and start oscillation. When the injection time exceeds the start time to oscillate, the electron beams will begin to bunching due to the increase of SPR intensity. When the beam-wave interaction meets the oscillation conditions, the net gain of the SPR satisfying the resonance conditions in the resonator will begin to increase gradually and finally establish the steady-state oscillation in the resonator. According to the resonance conditions, the resonator size must be reduced in order to increase the output frequency of the SP FEL based on rectangular grating. However, in the simulation of SP FEL, our group found that it was difficult to increase the output frequency of the SP FEL based on rectangular grating by reducing the resonator size. We also found that the grating grooves should be changed to increase the output frequency of the SP FEL.

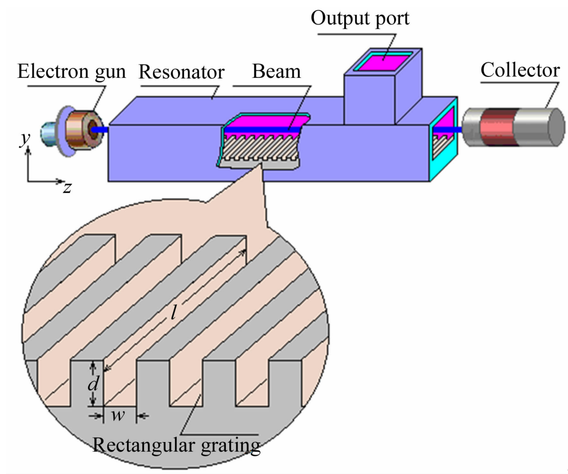

Fig. 1　Schematic diagram of the SP FEL based on rectangular grating

图 1　基于矩形光栅的 SP FEL 的原理图

3　Simulation and analysis of the SP FEL based on rectangular grating

In order to study the relationship between the size of grating and the output frequency of SP FEL, the characteristics of the SP FEL based on rectangular grating was studied by a Particle-In-Cell (PIC) simulation method. PIC software is mainly used to simulate the interaction of electromagnetic waves and space charges in the vacuum electronic device, and to calculate and analyze the complex electromagnetic problems involving space charges. It solves the electromagnetic problems by the Finite-Difference Time-Domain (FDTD) method to turn a problem in the continuous domain of electromagnetic field into a problem in the discrete system, that is, by using the numerical solutions at discrete points to approximate the real values in the continuous field domain. It is called by the FDTD because it differentiates the partial differential of time when solving the Maxwell's equations[23-26]. Through long-time development and improvement, the simulation result of PIC software has become a good fit to the experimental result, with a very small error between them. Therefore, this software is an ideal tool for the research on SP FEL characteristics.

3.1 Simulation parameter of the SP FEL based on rectangular grating

To generate strong coherent SPR during simulation, grating parameters (including the depth, length and width of grating groove), resonator parameters (including the length, width and height of resonator) and electron beam parameters must be optimized. The optimized resonator parameters and electron beam parameters are shown in Table 1[27-30]. According to the equation (1), the wavelength range of the spontaneous SPR fundamental wave corresponding to the parameters in Table 1 can be calculated to be from 1.026 9 mm (corresponding to the frequency 291.94 GHz) to 0.426 9 mm (corresponding to the frequency 702.18 GHz) in the THz band. The Fig. 2 shows the 3D simulation diagram of the SP FEL based on rectangular grating.

Tab.1 Resonator parameters and electron beam parameters of the SP FEL based on rectangular grating

表1 基于矩形光栅的 SP FEL 的谐振腔参数和电子束参数

Parameters	Value	Parameters	Value
Width of resonator/mm	1.5	Transverse size of beam/mm	0.5
Length of resonator/mm	36.9	Beam voltage/kV	50
Height of resonator/mm	0.75	Current/A	10

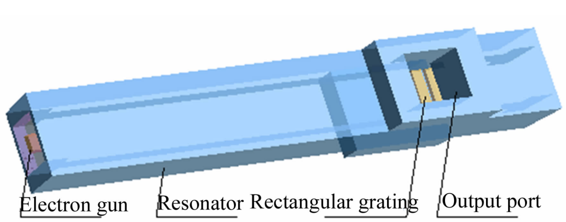

Fig. 2 Simulation graph of the SP FEL based on rectangular grating

图2 基于矩形光栅的 SP FEL 的模拟图

3.2 Simulation results of the SP FEL based on rectangular grating

The Fig. 3 shows the distribution of the kinetic energy of electron beams along the z-axis at different grating depths in the SP FEL. It can be seen from Fig. 3 that the electron beams in SP FEL are bunching remarkably at different depths of grating grooves, indicating that they have been obviously modulated. By calculating the spatial period of the pulsed electron string, it can be seen that the spatial period of the pulsed electron string increases with the increase of the depth of grating groove. Since the spatial period of the pulsed electron string is proportional to the operating wavelength of SP FEL, a larger depth of grating groove indicates a longer operating wavelength of SP FEL. The Fig. 4 shows the FFT spectra of SP FEL at different depths of grating groove. It can be seen from Fig. 4 that each FFT spectrum contains multiple spectral lines, which belong to two different types of radiation. One type of radiation or the radiation with the lower frequency originates from the diffraction emission of an evanescent wave and has the same frequency as the evanescent wave. The other type of radiation is the second harmonic of the evanescent wave. Judging from the amplitude of FFT spectrum, the second harmonic is just the output frequency of SP FEL. As can be seen from Fig. 4, the output frequency of SP FEL will decrease with the increase of grating groove depth. The Table 2 shows the simulated output frequencies of SP FEL at different depths of grating groove. As seen from the Table 2, the output frequency of SP FEL decreases with the increase of grating groove depth. It is worth noting that when the depth of grating groove is equal to 0.15 mm, the output frequency

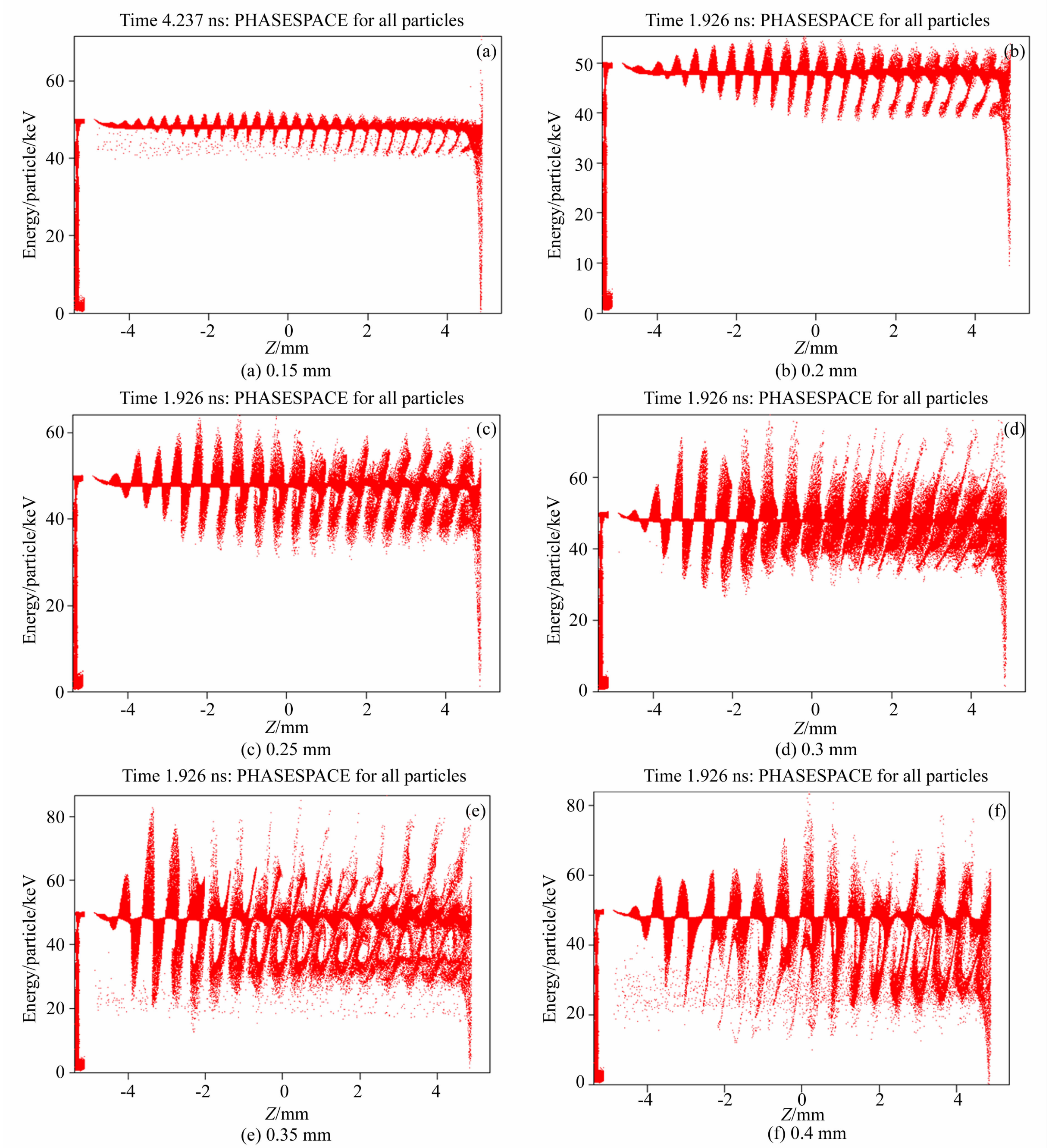

Fig. 3　Kinetic energy of beams in bunching state of SP FEL at different slot depths of grating

图 3　在不同光栅槽深时 SP FEL 中电子注的动能沿 z 轴分布图

of SP FEL will be 723.379 GHz, greater than the wavelength (702.18 GHz) of the spontaneous SPR fundamental wave. This is unexplained by equation (1). In addition, the output frequencies of SP FEL at different lengths and widths of grating groove have also been simulated. The Table 3 shows the simulated output frequencies of SP FEL at different lengths of grating groove. As seen from the Table 3, the output frequency of SP FEL decreases with the increase of grating groove length. The Table 4 shows the simulated output frequencies of SP FEL at different widths of grating groove. As seen from the Table 4, the output frequency of SP FEL decreases with the increase of grating groove width.

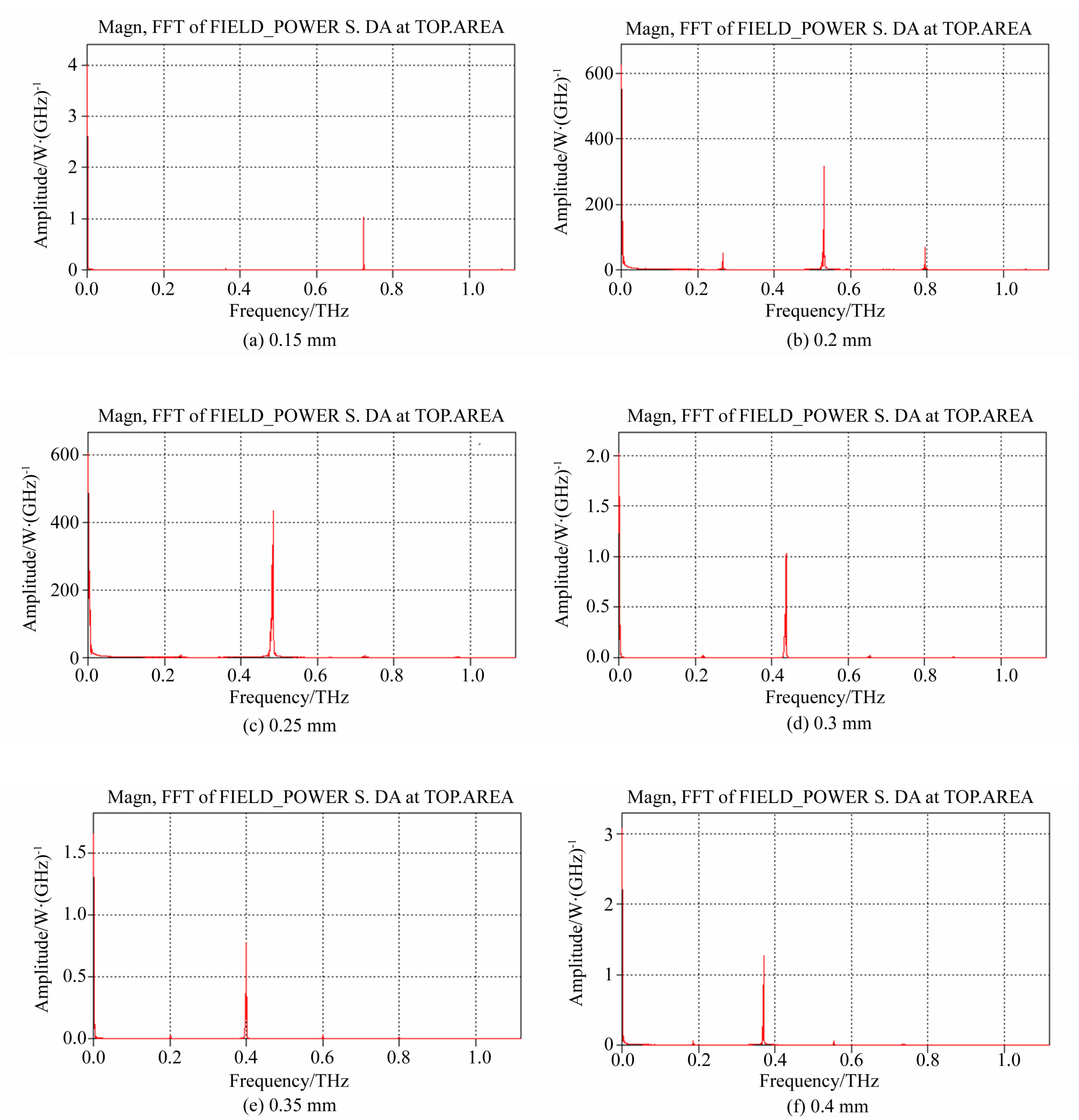

Fig. 4 Frequency spectra of the SP FEL at different depths of grating groove

图 4 在不同光栅槽深时 SP FEL 的频谱分布图

Tab. 2 Simulation values of output frequency of SP FEL at different depths of grating groove

表 2 在不同光栅槽深时 SP FEL 输出频率的模拟值

Parameters	Values					
Number of periods	32					
Period length of grating/mm	0.3					
Slot length of grating/mm	1.5					
Slot width of grating/mm	0.1					
Slot depth of grating/mm	0.15	0.2	0.25	0.3	0.35	0.4
Simulation value of output frequency / GHz	723.379	529.786	483.632	436.827	400.121	370.060

Tab. 3 Simulation values of output frequency of SP FEL at different lengths of grating groove

表 3 在不同光栅槽长时 SP FEL 输出频率的模拟值

Parameters	Values	
Number of periods	32	
Period length of grating/mm	0.3	
Slot width of grating/mm	0.1	
Slot depth of grating/mm	0.2	
Slot length of grating/mm	0.75	1.5
Simulation value of output frequency/GHz	727.255	529.786

Tab. 4 Simulation values of output frequency of SP FEL at different widths of grating groove

表 4 在不同光栅槽宽时 SP FEL 输出频率的模拟值

Parameters	Values		
Number of periods	32		
Period length of grating/mm	0.3		
Slot length of grating/mm	1.5		
Slot depth of grating/mm	0.2		
Slot width of grating/mm	0.1	0.15	0.2
Simulation value of output frequency / GHz	529.786	515.823	508.692

Tab. 5 Estimation values of LCR of grating groove at different groove depths

表 5 不同光栅槽深时光栅槽的 LCR 估算值

Slot depth of grating/mm	Estimation value of LCR/GHz
0.15	302.849
0.2	224.843
0.25	178.800
0.3	148.412
0.35	126.854
0.4	110.765

Tab. 6 Estimation values of LCR of grating groove at different groove lengths

表 6 不同光栅槽长时光栅槽的 LCR 估算值

Slot length of grating/mm	Estimation value of LCR/GHz
0.75	317.976
1.5	224.843

Tab. 7 Estimation values of LCR of grating groove at different groove widths

表 7 不同光栅槽宽时光栅槽的 LCR 估算值

Slot width of grating/mm	Estimation value of LCR/GHz
0.1	224.843
0.15	150.806
0.2	137.482

4 Analysis and estimation of rectangular grating

4.1 Analysis of rectangular grating

In order to explain the relationship between the output frequency of the SP FEL based on rectangular grating and the depth, length and width of grating groove, the grating structure needs to be studied[31-32]. Structurally, the grating grooves of the SP FEL based on rectangular grating are very similar to the anode cavities of a magnetron. As we all know, each anode cavity in a magnetron can be equivalent to an LC resonance circuit. For example, in the fan-shaped anode cavity, the groove of each anode cavity can be equivalent to a capacitor, while the metal portion of each anode cavity can be equivalent to an inductance. Since each anode cavity in a magnetron can be equivalent to an LC resonance circuit, each grating groove in SP FEL with the structure similar to anode cavity can also be equivalent to an LC resonance circuit. The parallel opposite parts of each rectangular grating groove can be equivalent to a parallel plate capacitor, whose capacitance can be expressed as

$$C = \frac{\varepsilon l d}{w}, \tag{2}$$

as shown in Fig. 1, l is the length of grating groove, referred to as grating groove length; d is the depth of grating groove, referred to as grating groove depth; and w is the width of grating groove, referred to as grating groove width. The metal portion of each rectangular grating groove can be equivalent to a U-shaped wire. The inductance of U-shaped wire is approximately expressed as

$$L \approx k_1 \frac{\mu w}{2\pi} + k_2 \frac{\mu d}{\pi}, \tag{3}$$

where k_1 and k_2 are constants; if $w \gg r$, then $k_1 = \ln \frac{2w}{r} - 0.75$, $k_2 = \ln \frac{w}{r} + 0.25$, r is current penetration depth. The higher the rate of current change, the smaller the current penetration depth. For copper conductors, when the current frequency reaches 4 GHz, the current penetration depth is already as small as 0.1 mm. If $w \approx r$, then $k_1 \neq \ln \frac{2w}{r} - 0.75$, $k_2 \neq \ln \frac{w}{r} + 0.25$. Since only the output frequency of SP FEL is estimated in the following text, $k_1 = \ln \frac{2w}{r} - 0.75$ and $k_2 = \ln \frac{w}{r} + 0.25$ will still be used to estimate the value of LC oscillatory Radiation (LCR).

Since each rectangular grating groove has capacitance and inductance, it is equivalent to an LC resonance circuit. The resonant frequency of LC resonance circuit is

$$f_0 = \frac{1}{2\pi\sqrt{LC}}. \tag{4}$$

The equations (2) and (3) are substituted into equation (4) to obtain the estimation equation of resonant frequency of each grating groove

$$f_0 \approx \frac{c}{\sqrt{2\pi}} \sqrt{\frac{w}{ld(k_1 w + 2k_2 d)}}. \tag{5}$$

The equation (5) indicates that the resonant frequency of each grating groove is related to the groove length l, the groove depth d and the groove width w.

In a magnetron, when the "electron spokes" sweep through the anode cavity, they will enable the charging and discharging and then the oscillation and the generation of electromagnetic waves in the anode cavity. The generated electromagnetic waves can continue to modulate the "electron spokes" and change the period of their rotation. When the rotation period of "electron spokes" matches the resonant period of anode cavity, electromagnetic resonance will occur, the net gain of electromagnetic waves will begin to increase gradually, and finally the steady-state oscillation will be formed and maximized.

In the SP FEL, the resonator surface can reflect the spontaneous SPR back into the electron beams for interaction, thus modulating the electron beam velocity. As the electron beams continue to move, their velocity modulation will be changed into their density modulation so that the electron beams will bunching and form pulsed electrons. These pulsed electrons resemble the "electron spokes" in a magnetron. When passing over the grating grooves, they can induce the charges on the grating. The induced charges will enable the charging and discharging and then the oscillation and the generation of electromagnetic waves in the LC resonance circuit corresponding to the grating grooves. The generated electromagnetic waves can continue to interact with the electron beams in the resonator and modulate the pulsed electrons, thus continuing to change their spatial period. When the spatial period of the pulsed electrons matches the resonant period of the LC resonance circuit formed by grating grooves, the net gain of SPR will start to increase gradually and finally form the steady state oscillation. Thus there are two kinds of radiation in SP FEL: SPR and LCR.

4.2 Estimation of LCR value of rectangular grating grooves

In order to explore the relationship between the output frequency of SP FEL and the LCR of grating grooves, the LCR values of the grating grooves at different depths are estimated according to the equation (5) and the parameters in Table 1 and Table 2, and the estimated results are shown in Table 5. The current penetration depth used for LCR estimation is 0.1 mm. By comparing the simulated values of SP FEL output frequency in Table 2 and the LCR estimations of grating grooves in Table 5, it can be seen that the simulated values of SP FEL output frequency at different groove depths are of the same order of magnitude as the LCR estimations of grating grooves. The reason for the large error between the simulated value of SP FEL output frequency and the LCR of grating groove estimated from equation (5) is that both inductance and current penetration depth are approximated. In spite of this error, both the simulated value of SP FEL output frequency and the estimated LCR value of grating groove will decrease with the increase of groove depth.

Likewise, the LCR values of the grating grooves at different lengths can be estimated according to the equation (5) and the parameters in Table 1 and Table 3, and the estimated results are shown in Table 6. The LCR values of the grating grooves at different widths can be estimated according to the equation (5) and the parameters in Table 1 and Table 4, and the estimated results are shown in Table 7. The current penetration depth used for LCR estimation is 0.1 mm. By comparing the simulated values of SP FEL output frequency in Table 3 and the LCR estimations of grating grooves in Table 6, it can be seen that the simulated values of SP FEL output frequency at different groove lengths are of the same order of magnitude as the LCR estimations of grating grooves. In addition, they will decrease with the increase of groove length. By comparing the simulated values of SP FEL output frequency in Table 4 and the LCR estimations of grating grooves in Table 7, it can be seen that the simulated values of SP FEL output frequency at different groove widths are of the same order of magnitude as the LCR estimations of grating grooves. In addition, they will decrease with the increase of groove width.

The simulated values of SP FEL output frequency at different grating sizes are of the same order of magnitude and in the same variation law with the LCR estimations of grating grooves. It is inferred that the output frequency of SP FEL is determined by the LCR of grating groove, rather than the SPR. That is, the output frequency of SP FEL is determined by grating grooves, rather than resonator. However, the resonator is indispensable. Similar to the central cavity of a magnetron, the resonator of SP FEL is also a space of beam-wave interaction that modulates the electron beams and enables them to bunching. As can be seen from Table 2, when the depth of grating groove is equal to 0.15 mm, the output frequency will be 723.379 GHz, greater than the maximum wavelength (702.18 GHz) of the spontaneous SPR fundamental wave. Thus it can be further inferred that the output radiation of SP FEL should be the LCR of grating grooves, rather than the SPR emitted by electron beams in a specific direction.

5 Conclusion

Through the above PIC simulation and theoretical analysis, it can be found that:

(1) The output frequency of SP FEL decreases with the increase in the depth, length and width of grating grooves;

(2) Each grating groove in SP FEL can be equivalent to an LC resonance circuit;

(3) There are two kinds of radiation in SP FEL: SPR and LCR;

(4) The simulated values of SP FEL output frequency at different grating sizes are of the same order of magnitude (10^2 GHz) and in the same variation law with the LCR estimations of grating grooves. Thus it can be inferred that the output frequency of SP FEL is determined by grating grooves, rather than resonator.

——中文对照版——

1 引 言

当电子束紧贴着周期性金属结构的表面飞行时,将激励起远红外、微米波、太赫兹波段的电磁辐射,这种现象被称为史密斯—帕塞尔(Smith-Purcell, SP)效应,这种辐射被称为史密斯—帕塞尔辐射(SPR)[1]。然而这种自发的SPR是非相干的,强度很弱,不容易检测和应用。为了获得相干的SPR,通常利用相对论电子束激励由开放式谐振腔(或封闭式谐振腔)作为反馈元件连同金属光栅组成的高频互作用系统,这种实验结构被称为史密斯—帕塞尔自由电子激光(Smith-Purcell Free-Electron Laser, SP FEL)[2-5]。SP FEL已经成功地在远红外、微米波、太赫兹波段进行了实验[6-9]。这些实验为开发远红外、微米波、太赫兹波段光源呈现出美好前景,已成为国内外太赫兹(THz,0.1~10 THz)源研究的热点之一,是开发大功率、高频率、可调谐、更紧凑、更简单、低成本THz源的一种极有前途的选择。

为了获得大功率的SP FEL,近几年研究者在优化谐振腔、电子束和光栅等方面开展了研究。其中在谐振腔优化方面,研究发现类似于Orotron的开放腔体结构可以将辐射功率提高2个数量级以上[6]。其THz区域的平均输出功率可以达到数百毫瓦甚至数瓦特,比传统的Orotron高出许多个数量级。在电子束优化方面,主要利用预聚束来提高SPR的频率和功率。2007年,史宗君、杨梓强等人发现使用预聚束不仅可以激发相干SPR,也可以获得期望的SPR频率和功率,例如,当一束预聚束的电子束通过接近金属光栅的表面时,就能够获得相干的SPR[10]。通过正确选择参数,就可以产生极强的窄带THz辐射。2016年,Kumar P等人报道了利用激光调制的电子束在金属光栅上产生了SP THz辐射[11]。在光栅优化方面,主要通过改进光栅的形状和结构来提高SPR。2015年,Naumenko等人报道了一种基于凹面光栅的SPR,发现凹面光栅可以显著增加相干SPR的空间密度。同年,Zhang P等人也报道了一种增强相干的THz波段SPR。他们通过优化光栅,预聚束和开放式谐振腔来产生增强相干的THz波段SPR。此外,他们还发现通过优化光栅参数,改变光栅的凹槽宽度和高度可以减小起振电流数量级[12]。他们还研究了一种基于光栅凹槽阵列的增强THz波段SPR。这种SPR功率比电子通过非常接近光栅表面的情况高十倍[13]。2016年,刘维浩,陆亚林等人提出了一种基于两个串联圆柱形光栅的改进SP FEL。这种改进SP FEL能够增加辐射频率,辐射功率也能够提高几十倍[14-16]。综上所述,可以看出在SP FEL研究中,对光栅尺寸和SP FEL输出频率间关系的研究一直是一个空白,为此本文以基于矩形光栅的SP FEL为例,研究了光栅尺寸和SP FEL输出频率之间的关系。

2 基于矩形光栅的SP FEL的结构与原理

基于矩形光栅的SP FEL结构如图1所示。它由电子枪、谐振腔、矩形光栅和集电极组成。在该装置中,在谐振腔底部有一个矩形光栅,矩形光栅的光栅槽与x方向平行,矩形光栅和谐振腔都由导电良好的金属材料(如无氧铜)制成,因此矩形光栅和谐振腔的表面可以认为是理想导体。位

于光栅左边的阴极(电子枪)能够产生一束沿 z 轴传播的电子束。当电子束紧贴矩形光栅的表面运动时,在光栅表面上会感应出大量电荷,在光栅附近就存在周期性电场,电子束在运动中就会受到周期性电场的作用,于是发出 SPR。SPR 的波长:

$$\lambda = \frac{D}{n}\left(\frac{1}{\beta} - \cos\theta\right), \tag{1}$$

其中 D 为光栅周期、n 为空间谐波数,θ 为发射角(即 SPR 与电子运动方向的夹角),$\beta = v/c$ 为电子运动速度与光速之比。根据式(1),自发的 SPR 基波的波长范围从 $D\left(\frac{1}{\beta}-1\right)$到 $D\left(\frac{1}{\beta}+1\right)$[17-22]。传统 SP FEL 理论认为,谐振腔的表面能够将各种波长的 SPR 反射回电子束,反射回的 SPR 对电子束进行调制。但是在电子束注入初期,SPR 的强度不足以引起电子束群聚,不能起振。当注入时间超过起振时间时,由于 SPR 的强度增强,电子束开始群聚。当注-波互作用达到受激条件时,谐振器中的满足谐振条件的 SPR 的净增益就开始逐渐增大,并最终在谐振器中建立起稳态振荡,根据谐振腔的谐振条件,人们一直认为要提高基于矩形光栅的 SP FEL 的输出频率就要减小谐振腔的尺寸。但本项目组在 SP FEL 的模拟中发现减小谐振腔的尺寸,很难提高基于矩形光栅的 SP FEL 的输出频率,并发现要提高 SP FEL 输出频率,必须改变光栅槽。

3　基于矩形光栅的 SP FEL 的模拟与分析

为了研究光栅尺寸和 SP FEL 输出频率之间的关系,利用粒子模拟(Particle-In-Cell, PIC)软件对基于矩形光栅的 SP FEL 的特性进行三维模拟。PIC 软件主要用于模拟电真空器件中电磁波与空间电荷的互作用过程,计算和分析有空间电荷存在的复杂电磁问题。它是利用时域有限差分法(Finite-Difference Time-Domain, FDTD),把电磁场连续域内的问题变为离散系统的问题再求解电磁问题的,即用各离散点上的数值解来逼近连续场域内的真实值。由于它在求解 Maxwell 方程组时,将对时间的偏微分也进行差分,所以被称作时域有限差分法[23-26]。PIC 软件经过长期的发展和改进,模拟结果与实验结果非常吻合,误差很小,是进行 SP FEL 的特性研究的理想工具。

3.1　基于矩形光栅的 SP FEL 的模拟参数

在进行模拟时,为了获得较强的相干的 SPR,光栅参数(包括光栅槽深、光栅槽长、光栅槽宽)、谐振腔参数(包括长度、宽度、高度)和电子束参数都必须是最优的。经过优化后的谐振腔参数和电子束参数如表 1 所示[27-30]。根据式(1),可以计算出表 1 参数对应的自发 SPR 基波的波长范围为从 1.026 9 mm(对应频率为 291.94 GHz)到 0.426 9 mm(对应频率为 702.18 GHz),处于太赫兹波段。图 2 给出了基于矩形光栅的 SP FEL 的三维模拟图。

3.2　基于矩形光栅的 SP FEL 的模拟结果

图 3 给出了 SP FEL 在不同光栅槽深时电子束的动能沿 z 轴分布图。从图 3 可以看出,SP FEL 在不同光栅槽深时都存在明显的群聚现象,这说明电子束都受到了明显的调制。通过计算脉冲电子串的空间周期,可以看出光栅槽深越大,脉冲电子串的空间周期越大。由于电子串的空间周期对应 SP FEL 的工作波长,这说明光栅槽深越大, SP FEL 的工作波长越大。图 4 给出了 SP FEL 在不同光栅槽深时的 FFT 谱。从图 4 可以看出每个 FFT 谱中都存在多条谱线,这些属于两种不同类型的辐射。频率最低的一种是源于倏逝波的衍射发射,其频率为倏逝波的频率。另一种对应于倏逝波的二次谐波。从 FFT 谱的幅度来看,该二次谐波就是 SP FEL 的输出频率。从图 4 可以看出,光栅槽深越大,SP FEL 的输出频率越小。表 2 给出了在不同光栅槽深时 SP FEL 输出频率的模拟值。其规律是 SP FEL 的输出频率随光栅槽深的增大而减小。值得注意的是,当光栅槽深等于0.15 mm时,SP FEL 的输出频率是 723.379 GHz,大于自发 SPR 基波的波长范围 702.18 GHz。这是式(1)不能解释的。此外,还模拟了不同光栅槽长、不同光栅槽宽时的 SP FEL 输出频率。表3 给出了在不同光栅槽长时 SP FEL 输出频率的模拟值。其规律是 SP FEL 的输出频率随光栅槽长的增大而减小。表 4 给出了在不同光栅槽宽时 SP FEL

输出频率的模拟值,其规律是 SP FEL 的输出频率随光栅槽宽的增大而减小。

4 矩形光栅的分析与估算

4.1 矩形光栅的分析

为了解释基于矩形光栅的 SP FEL 的输出频率与光栅槽的光栅槽深、光栅槽长、光栅槽宽的关系,需要从结构上研究光栅[31-32]。从结构上看,基于矩形光栅的 SP FEL 的光栅槽与磁控管的阳极谐振腔非常相似。众所周知,在磁控管中,每一个阳极谐振腔都可以等效为一个 LC 谐振电路。以槽扇型阳极谐振腔为例,其槽部分可以等效为一个电容,而其扇形部分可以等效为一个电感。既然磁控管中的阳极谐振腔可以等效为一个 LC 谐振电路, 结构上与之类似的 SP FEL 的光栅槽也可以等效为一个 LC 谐振电路。其中每个矩形光栅槽的平行正对部分可以等效为一个平行板电容器,其电容可以表示为:

$$C = \frac{\varepsilon l d}{w}, \tag{2}$$

如图 1 所示, l 是指光栅槽的缝隙长度,简称光栅槽长;d 是指光栅槽的缝隙深度,简称光栅槽深;w 是指光栅槽的缝隙宽度,简称光栅槽宽。每个矩形光栅槽的金属部分均可以等效为一个 U 形导线。对于 U 形导线,其电感可近似表示为:

$$L \approx k_1 \frac{\mu w}{2\pi} + k_2 \frac{\mu d}{\pi}, \tag{3}$$

其中 k_1 和 k_2 为常数,当 $w \gg r$ 时,$k_1 = \ln \frac{2w}{r} - 0.75$,$k_2 = \ln \frac{w}{r} + 0.25$, r 是电流透入深度,电流变化率越大, 电流透入深度越小。对于铜导体,当电流频率达到4 GHz时,电流透入深度已经小到 0.1 mm。当 $w \approx r$, $k_1 \neq \ln \frac{2w}{r} - 0.75$, $k_2 \neq \ln \frac{w}{r} + 0.25$,由于在下文中只是对 SP FEL 输出频率进行估算,因此仍然采用 $k_1 = \ln \frac{2w}{r} - 0.75$, $k_2 = \ln \frac{w}{r} + 0.25$。

由于每个矩形光栅槽都具有电容和电感,因此,每个光栅槽都相当于一个 LC 谐振电路。LC 谐振电路的谐振频率为:

$$f_0 = \frac{1}{2\pi\sqrt{LC}}, \tag{4}$$

将式(2)、式(3)代入式(4)得到光栅槽的谐振频率估算公式:

$$f_0 \approx \frac{c}{\sqrt{2\pi}} \sqrt{\frac{w}{ld(k_1 w + 2k_2 d)}}. \tag{5}$$

式(5)说明,每个光栅槽的谐振频率与光栅槽长 l、光栅槽深 d、光栅槽宽 w 都有关系。

在磁控管中,当“电子轮辐”扫过阳极谐振腔时,会对阳极谐振腔充放电,从而使阳极谐振腔振荡并产生电磁波。产生的电磁波可以继续调制“电子轮辐”并改变其旋转周期。当“电子轮辐”的旋转周期与阳极谐振腔的谐振周期匹配时,发生电磁谐振,电磁波的净增益就开始逐渐增大,并最终形成稳态振荡,达到最大值。

在 SP FEL 中,谐振腔的表面能够将自发的 SPR 反射回电子束,使电子束与 SPR 互作用,从而对电子束的速度进行调制。在电子束继续运动的过程中,电子束的速度调制就会转变为电子束的密度调制,使电子束发生群聚,形成脉冲电子串。这些脉冲电子串就类似磁控管中的“电子轮辐”。当它们在光栅槽上方运动时,它们能在光栅上感应出电荷,感应电荷会迫使光栅槽对应的 LC 谐振电路充放电,从而使光栅槽对应的 LC 谐振电路振荡并产生电磁波,产生的电磁波可以继续与谐振腔中的电子束互作用,并继续调制脉冲电子串,从而继续改变其空间周期。当脉冲电子串的空间周期与光栅槽形成的 LC 谐振电路的谐振周期匹配时,SPR 的净增益就开始逐渐增大,并最终形成稳态振荡。可见, 在 SP FEL 中存在两种辐射,除了 SPR,还有 LC 振荡辐射(LCR)。

4.2 矩形光栅槽 LCR 值的估算

为了探索史密斯—帕塞尔自由电子激光输出频率与光栅槽的 LCR 的关系,下面按照式(5)和表 1 和表 2 参数估算不同光栅槽深时光栅槽的 LCR 值,估算结果如表 5。其中估算 LCR 值时电流透入深度值取 0.1 mm。比较表 2 中的 SP FEL 输出频率的模拟值和表 5 中的光栅槽的 LCR 估算值,可以看出不同光栅槽深时 SP FEL 输出频率的模拟值与光栅槽的 LCR 估算值具有相同的数量级。SP FEL 输出频率的模拟值与根据式(5)估

算的光栅槽的 LCR 估算值误差较大的原因是由于电感和电流透入深度都用了近似值,虽然 SP FEL 输出频率的模拟值与根据式(5)估算的光栅槽的 LCR 估算值均存在误差,但都随光栅槽深的增大而减小,具有相同的变化规律。

同样按照式(5)和表 1 和表 3 参数可以估算不同光栅槽长时光栅槽的 LCR 值,估算结果如表 6。按照式(5)和表 1 和表 4 参数可以估算不同光栅槽宽时光栅槽的 LCR 值,估算结果如表 7。其中估算 LCR 值时电流透入深度值取 0.1 mm。比较表 3 中的 SP FEL 输出频率的模拟值和表 6 中的光栅槽的 LCR 估算值,可以看出不同光栅槽长时 SP FEL 输出频率的模拟值与光栅槽的 LCR 估算值具有相同的数量级,并且都随光栅槽长的增大而减小,具有相同的规律。比较表 4 中的 SP FEL 输出频率的模拟值和表 7 中的光栅槽的 LCR 估算值,可以看出不同光栅槽宽时 SP FEL 输出频率的模拟值与光栅槽的 LCR 估算值具有相同的数量级,并且都随光栅槽宽的增大而减小,具有相同的规律。

基于不同光栅尺寸时 SP FEL 输出频率的模拟值都与光栅槽的 LCR 估算值在数量级上和变化规律上一致,由此推测决定 SP FEL 输出频率的应该是光栅槽的 LCR,而不是 SPR。即决定 SP FEL 的输出频率的应该是光栅槽,而不是谐振腔。但是谐振腔不可缺少,谐振腔的作用类似磁控管的中心腔,也是一个注—波互作用空间,起着对电子束进行调制、使电子束发生群聚的作用。从表 2 可以看出,当光栅槽深等于 0.15 mm 时,输出频率是 723.379 GHz,大于自发 SPR 基波的波长范围 702.18 GHz,这进一步可以推测 SP FEL 的输出频率应该是光栅槽的 LCR,而不是电子束在特定方向上发射的 SPR。

5 结 论

通过上述 PIC 模拟和理论分析可发现:(1) SP FEL 的输出频率随着光栅槽深、光栅槽长、光栅槽宽的增大而减少;(2) SP FEL 中每个光栅槽都可以等效为一个 LC 谐振电路;(3) 在 SP FEL 中存在两种辐射,除了 SPR,还有 LCR;(4) 基于不同光栅尺寸时 SP FEL 输出频率的模拟值都与光栅槽的 LCR 估算值的数量级均为 10^2 GHz,且变化规律上一致。由此推测决定 SP FEL 输出频率的应该是光栅槽,而不是谐振腔。

参考文献:

[1] SMITH S J, PURCELL E M. Visible light from localized surface charges moving across a grating[J]. *Physical Review*, 1953, 92(4): 1069.

[2] GREEN B, KOVALEV S, ASGEKAR V, *et al*.. High-field high-repetition-rate sources for the coherent THz control of matter[J]. *Scientific Reports*, 2016, 6: 22256.

[3] MENG X ZH, WANG M H, ZHANG L M, *et al*.. Characteristic analysis of a Smith-Purcell terahertz source[J]. *Photonics Research*, 2016, 4(5): 162-167.

[4] 孟现柱, 王明红, 孙桂芳, 等. 基于微型谐振腔的史密斯-帕赛尔自由电子激光[J]. 聊城大学学报(自然科学版), 2018, 31(4): 48-51.
MENG X ZH, WANG M H, SUN G F, *et al*.. Smith-Purcell free electron laser based on micro-resonator[J]. *Journal of Liaocheng University (Natural Science Edition)*, 2018, 31(4): 48-51. (in Chinese)

[5] 孟现柱, 王明红, 张黎明, 等. 基于史密斯——帕赛尔效应的太赫兹振荡器的原理与特性分析[J]. 光子学报, 2016, 45(4): 0423003.
MENG X ZH, WANG M H, ZHANG L M, *et al*.. Principle and characteristics analysis of a terahertz oscillator based on Smith-Purcell effect[J]. *Acta Photonica Sinica*, 2016, 45(4): 0423003. (in Chinese)

[6] LIU W H, LU Y L, WANG L, *et al*.. A multimode terahertz-Orotron with the special Smith-Purcell radiation[J]. *Applied Physics Letters*, 2016, 108(18): 183510.

[7] LI D, IMASAKI K, YANG Z. Three-dimensional simulation of super-radiant Smith-Purcell radiation[J]. *Applied Physics Letters*, 2006, 88(20): 201501.

[8] ZHOU Y C, ZHANG Y X, LIU SH G. Electron-beam-driven enhanced terahertz coherent Smith-Purcell radiation within a cylindrical quasi-optical cavity[J]. *IEEE Transactions on Terahertz Science and Technology*, 2016, 6(2): 262-267.

[9] 史宗君, 唐效频, 兰峰, 等. 太赫兹频段一维介质光子晶体中的史密斯-帕塞尔辐射特性模拟[J]. 红外与毫米波学报, 2014, 33(2): 183-187.

SHI Z J, TANG X P, LAN F, *et al*.. Simulation of terahertz Smith-Purcell radiation from one-dimensional dielectric photonic crystal[J]. *Journal of Infrared and Millimeter Waves*, 2014, 33(2): 183-187. (in Chinese)

[10] LI W W, XU Y F, LU Y L, *et al*.. Enhancement of coherent THz Smith-Purcell radiation by resonance overlapping[J]. *Journal of Infrared, Millimeter, and Terahertz Waves*, 2017, 38(1): 12-21.

[11] KUMAR P, BHASIN L, TRIPATHI V K, *et al*.. Smith-Purcell terahertz radiation from laser modulated electron beam over a metallic grating[J]. *Physics of Plasmas*, 2016, 23(9): 093301.

[12] ZHANG P, ANG L K, GOVER A. Enhancement of coherent Smith-Purcell radiation at terahertz frequency by optimized grating, prebunched beams, and open cavity[J]. *Physical Review Special Topics- Accelerators and Beams*, 2015, 18(2): 020702.

[13] ZHANG P, ZHANG Y, TANG M. Enhanced THz Smith-Purcell radiation based on the grating grooves with holes array[J]. *Optics Express*, 2017, 25(10): 10901-10910.

[14] 刘维浩, 陆亚林, 贾启卡. 一种基于特异 Smith-Purcell 效应的太赫兹辐射源: 中国, CN201610220733.5[P]. 2016-08-03.

LIU W H, LU Y L, JIA Q K. Terahertz radiation source based on special Smith-Purcell effect: CN, CN201610220733.5[P]. 2016-08-03. (in Chinese)

[15] 刘维浩, 梁林波, 陆亚林, 等. 基于两段矩形光栅的史密斯-帕赛尔电磁辐射源: 中国, CN201710347815.0[P]. 2017-05-07.

LIU W H, LIANG L B, LU Y L, *et al*.. Smith passail electromagnetic radiation source based on two rectangular grating: CN, CN201710347815.0[P]. 2017-05-07. (in Chinese)

[16] LIANG L B, LIU W H, JIA Q K, *et al*.. High-harmonic terahertz Smith-Purcell free-electron-laser with two tandem cylindrical-gratings[J]. *Optics Express*, 2017, 25(3): 2960-2968.

[17] LIU W X, TANG CH X, HUANG W H. Characteristics of terahertz coherent transition radiation generated from picosecond ultrashort electron bunches[J]. *Chinese Physics B*, 2010, 19(6): 062902.

[18] CHEN J Y, ZHENG L, ZHANG Y CH, *et al*.. A novel Smith-Purcell free electron laser[J]. *International Journal of Electronics*, 2011, 88(4): 467-471.

[19] KUMAR P, BHASIN L, TRIPATHI V K, *et al*.. Smith-Purcell terahertz radiation from laser modulated electron beam over a metallic grating[J]. *Physics of Plasmas*, 2016, 23(9): 093301.

[20] ZHANG Y X, DONG L. Enhanced coherent terahertz Smith-Purcell superradiation excited by two electron-beams[J]. *Optics Express*, 2012, 20(20): 22627-22635.

[21] BEI H, DAI D D, DAI ZH M. Simulation of Smith-Purcell radiation from compact terahertz source[J]. *High Power Laser and Particle Beams*, 2008, 20(12): 2067-2072.

[22] GAO X, YANG Z Q, QI L M, *et al*.. Three-dimensional simulation of a Ka-band relativistic Cherenkov source with metal photonic-band-gap structures[J]. *Chinese Physics B*, 2009, 18(6): 2452-2458.

[23] 席阳红, 谢国大, 徐辉, 等. 时变磁化等离子体的 LTJEC-FDTD 方法研究[J]. 发光学报, 2018, 39(7): 1029-1035.

XI Y H, XIE G D, XU H, *et al*.. Analysis of time-varying magnetic plasma by using LTJEC-FDTD method[J]. *Chinese Journal of Luminescence*, 2018, 39(7): 1029-1035. (in Chinese)

[24] 李传起, 范庆斌, 陆叶, 等. 多信道异质结构光子晶体滤波器[J]. 光学 精密工程, 2015, 23(8): 2171-2177.

LI CH Q, FAN Q B, LU Y, *et al*.. Multi-channel heterophotonic crystal filter[J]. *Opt. Precision Eng.*, 2015, 23(8): 2171-2177. (in Chinese)

[25] 杨波, 梁静秋, 梁中翥, 等. 液晶-金属光子晶体波导的光学特性[J]. 发光学报, 2011, 32(11): 1159-1164.

YANG B, LIANG J Q, LIANG ZH ZH, *et al*.. The optical properties of a liquid crystal-metal photonic crystal waveguide [J]. *Chinese Journal of Luminescence*, 2011, 32(11): 1159-1164. (in Chinese)

[26] 刘杰, 铁生年, 卢辉东. 多信道二维光子晶体滤波器[J]. 光学 精密工程, 2016, 24(5): 1021-1027.
LIU J, TIE SH N, LU H D. Multi-channel drop filter based on two-dimensional photonic crystal[J]. *Opt. Precision Eng.*, 2016, 24(5): 1021-1027. (in Chinese)

[27] MENG X ZH. Smith-Purcell free electron laser based on a semi-conical resonator[J]. *Optics Communications*, 2012, 285(6): 975-979.

[28] MENG X ZH. Smith-Purcell free electron laser based on a multilayer metal-dielectric stack[J]. *Optik - International Journal for Light and Electron Optics*, 2013, 124(17): 3162-3164.

[29] MENG X ZH, WANG M H, REN ZH M. Smith-Purcell free electron laser based on the semi-elliptical resonator[J]. *Chinese Physics B*, 2011, 20(5): 050702.

[30] MENG X ZH, WANG M H, REN ZH M. Smith-Purcell radiation in a grating-resonator composite structure[J]. *Journal of Infrared and Millimeter Waves*, 2016, 35(1): 21-24.

[31] 王雪飞, 卢振武, 王泰升, 等. 超表面上表面等离激元波的光栅衍射行为研究[J]. 中国光学, 2018, 11(1): 60-73.
WANG X F, LU ZH W, WANG T SH, *et al*.. Grating diffractive behavior of surface Plasmon wave on meta-surface[J]. *Chinese Optics*, 2018, 11(1): 60-73. (in Chinese)

[32] 刘镜, 刘娟, 王涌天, 等. 亚波长金属光栅的表面等离子体激元共振特性[J]. 中国光学, 2011, 4(4): 363-368.
LIU J, LIU J, WANG Y T, *et al*.. Resonant properties of sub-wavelength metallic gratings[J]. *Chinese Optics*, 2011, 4(4): 363-368. (in Chinese)

作者简介:

MENG Xian-zhu(1968—), male, born in Pingyi County, Shandong Province. Professor, master supervisor. He graduated from Liaocheng Teacher's University in 1991 and obtained his master's degree from Shandong Normal University in 2002. Now he is a professor of Liaocheng University and is mainly engaged in the research of free electron laser. E-mail: mengxz@lcu.edu.cn

孟现柱(1968—),男,山东平邑人,教授,硕士生导师,1991 年于聊城师范学院获得学士学位,2002 年于山东师范大学获得硕士学位,现为聊城大学教授,主要从自由电子激光的研究。E-mail: mengxz@lcu.edu.cn